Lung Deformation Estimation and Four-Dimensional CT Lung Reconstruction

Sheng Xu[1], Russell H. Taylor[1], Gabor Fichtinger[1], and Kevin Cleary[2]

[1] Engineering Research Center, Johns Hopkins University,
Baltimore, MD 21218, MD USA
{sheng, rht, gabor}@cs.jhu.edu
[2] Imaging Science and Information Systems (ISIS) Center, Department of Radiology,
Georgetown University Medical Center, Washington, DC 20007, USA
cleary@georgetown.edu

Abstract. Four-dimensional (4D) computed tomography (CT) image acquisition is a useful technique in radiation treatment planning and interventional radiology in that it can account for respiratory motion of lungs. Current 4D lung reconstruction techniques have limitations in either spatial or temporal resolution. In addition, most of these techniques rely on auxiliary surrogates to relate the time of CT scan to the patient's respiratory phase. In this paper, we propose a novel 4D CT lung reconstruction and deformation estimation algorithm. Our algorithm is purely image based. The algorithm can reconstruct high quality 4D images even if the original images are acquired under irregular respiratory motion. The algorithm is validated using synthetic 4D lung data. Experimental results from a swine study data are also presented.

1 Introduction

In radiation oncology, 4D CT is one technique that can account for respiratory motion during treatment planning. 4D CT may allow for the reduction of target volume margin to achieve increased tumor dose and decreased normal tissue dose [1]. While the radiation dose to the patient may be an issue, particularly if multiple 4D datasets are considered, in general the CT dose will be much less than the treatment dose delivered during radiation therapy. 4D CT may also be used to investigate the motion correlation between the internal tumor and external fiducials such as skin markers. The tumor position could then be estimated during the treatment by tracking the external fiducials. With sufficient 4D CT datasets, a respiratory model might also be constructed to parameterize the respiratory motion.

Most 4D lung reconstruction algorithms reported in the literature can be grouped into the following two approaches. The first approach requires controlling the patient's breath during image acquisition [2]. The respiratory cycle is divided into several phases (usually 7-11). The respiration is halted in each phase while a 3D CT volume is taken. A related technique is to use breathing tracking strategies such as active breathing control [3], [4], [5] to monitor the patient's breath at each phase. The 4D data acquired by this method has high spatial resolution, but very poor temporal resolution. This low temporal resolution limits its usefulness in analyzing the anatomical motion.

J. Duncan and G. Gerig (Eds.): MICCAI 2005, LNCS 3750, pp. 312 – 319, 2005.

The second approach does not try to monitor or control the patient's breath. The patient is allowed to breath freely on the CT table [2], [7]. The table is moved in small increments and a continuous free CT scan is taken at each table position to cover at least one complete respiratory cycle. Some external devices may be used during the scan to synchronize the CT scanning time with the respiratory phase [6], [7]. After image acquisition, all the free scan images are sorted into a sequence of 3D volumes according to their respiratory phase and table positions. This method has high temporal resolution at each table position. The major problem with this method is that respiratory motion is not completely repeatable, so the time stamp of the free scan image may not correlate well with the regular respiratory motion. In such a case, the image quality of the 3D data reconstructed at each respiratory phase will be very poor. It is usually very difficult to stitch these 3D volumes together into a 4D dataset.

Unlike prior methods, we propose a new 4D lung reconstruction method that has good temporal resolution and high reconstruction quality. In addition, our method does not rely on any external gating / tracking devices to synchronize the time of CT scan and the respiratory phase. Therefore problems caused by the discrepancy between the respiratory motion and the auxiliary surrogates are avoided.

2 Method

The outline of our 4D CT lung reconstruction method is as follows. First, a reference 3D CT volume is obtained under a long breath hold. Next, a continuous scan is taken at every table position to obtain a series of 2D images, while the patient is breathing freely. The 2D image series at every table position covers at least one complete respiratory cycle. Using deformable registration, each 2D image is registered to the reference volume to estimate the displacement field of the 2D image with respect to the reference volume. The respiration signal is extracted from the displacement field of each 2D image. This respiration signal is used to synchronize the 2D image series to the respiratory cycle at every table position. After the synchronization, the displacement field for the entire lung volume at every selected respiratory phase is reconstructed, interpolated and smoothed. The 4D lung images are reconstructed by a deformable transformation of the reference volume for the entire respiratory cycle.

2.1 Registration of 2D Image to Reference CT Volume

To calculate the deformation of the 2D image with respect to the reference volume, we divide the 2D image into small overlapping disk regions, and register each of the small regions piece by piece to the reference volume. The local registration algorithm is based on minimizing the Zero Mean Sum of Squared Differences (ZSSD) between a small region in the 2D image and a corresponding one in the reference volume. Quadratic transformation is used to model the deformation between the two regions. As a result, thirty parameters are estimated while the objective function is optimized. The details of the local registration are described in [8].

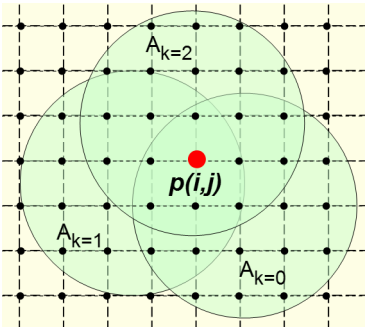

Fig. 1. Propagation of local registration

Since the registrations are performed at each local region, there is no guarantee that all the local registrations converge correctly. A global regularization of the registrations is necessary to remove outliers. In an example shown in Fig. 1, the regions are partially overlapped on each other. Since pixel p is included in all the disk regions A0, A1 and A2, the deformation of pixel p can be calculated from every one of these regions. As shown in equation (1), the final deformation of pixel p is the weighted average of all deformations obtained from the overlapped regions.

$$\hat{d}(i,j) = \sum_k r_k c_k w_k(i,j) d_k(i,j) \tag{1}$$

where d_k is the pixel displacement obtained from the kth region; $\hat{d}$ is the weighted average of the displacement; r_k is a function of the registration error of kth region. r_k will be assigned a large value for small registration error, and vice versa. r_k will be zero if the registration error of a region is above a threshold. c_k is a function of the registration consistency in the overlapping area between the current region k and the previously registered region. c_k will be large if the consistency is high, otherwise c_k will be small. c_k will be zero if the difference between current registration results and the previous registration results is too large. The assumption is that the results from previous registrations are more likely to be correct, because they are the weighted averages of many local registrations. w_k is a Gaussian window function that is centered on the center of region k, allowing the registration results of central pixels to have larger weight. As a result, Equation (1) filters out failed and bad registrations, and assigns large weight to good registrations. Unlike other registration techniques going from coarse to fine resolution, this registration goes from local to global. The algorithm iteratively propagates its local registrations, allowing the regions without enough local texture to be correctly estimated. This is an advantage over the spline-based registration [9] methods that rely on the local information of the control points. This procedure also makes the displacement field of the whole lung very smooth.

The region-based algorithm assumes the pixels of the region to have approximately the same type of motion. It is necessary that all the pixels in the region are lung pixels. If the region includes other pixels such as heart pixels (Fig.2 (b)), the registration is prone to fail, because the selected deformation models cannot explain the pixel motion of the analysis window. For the same reason, the region cannot have chest wall pixels (Fig.2 (a)), nor can the region have pixels from both the left and right lungs (Fig.2 (c)). Therefore, accurate lung segmentation is necessary before the registration, and the left and right lungs should be separated in the 2D images.

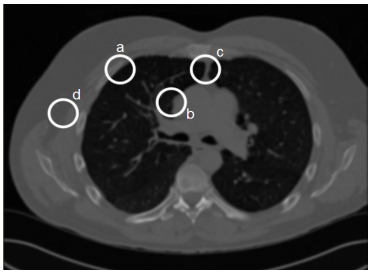

Fig. 2. Undesired regions: (a) both lung pixels and chest-wall pixels are included; (b) both lung pixels and heart pixels are included; (c) both left and right lungs are included (d) non-lung pixels are included

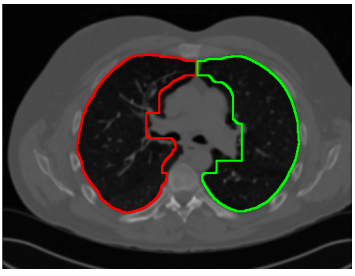

Fig. 3. The result of lung segmentation. Note that (a) the blood vessels are preserved; (b) the heart and chest-wall are removed; (c) the left and right lungs are separated; and (d) the marginal pixels are removed from the heart-lung boundary.

We adopted the techniques of Hu [10] to automatically segment the lungs in the 2D image. Base on their work, morphological closing is executed on the lung area to keep the small to middle blood vessels in the lungs. Extra margin is also introduced in the heart-lung boundary to exclude the artifact caused by the cardiac motion. The result of lung segmentation is shown in Figure 3.

2.2 Four-Dimensional Lung Reconstruction

After all the 2D images are registered to the preoperative lung volume, the average deformation of each image with respect to the reference volume is calculated, yielding a 3D motion vector. For the images taken at the same table position, a sequence of motion vectors is obtained. This vector sequence can be used as the respiration signal to synchronize the 2D image series at different table positions. It is assumed that there is no phase difference of respiratory motion in the craniocaudal direction. Since the tumor's respiratory motion is limited in a few centimeters, this assumption is valid. As a result, the two sequences of motion vectors at two adjacent table positions can be correlated to synchronize the scanning time at the two table positions with respect to the respiratory phase. The correlation is calculated using the following formula:

$$S = \arg\max_{j} \sum_{k=0}^{N-1} \left(\Delta x_k \Delta x'_{j+k} + \Delta y_k \Delta y'_{j+k} + \Delta z_k \Delta z'_{j+k} \right) \tag{2}$$

where N is the total number of frames to be correlated; $(\Delta x_k, \Delta y_k, \Delta z_k)$ is the average deformation of the k^{th} 2D image at the a table position; $(\Delta x'_k, \Delta y'_k, \Delta z'_k)$ is the average deformation for the k^{th} image at another table position; S is the number of frame shift between the two image sequences. By repeating this procedure at all table positions, all the 2D images can be synchronized.

Using principal component analysis, the principal axis of the motion trajectory can be obtained. By projecting the average motion on the principal axis, the one-dimensional respiration signal can be extracted. Fig. 4 shows the extracted respiration

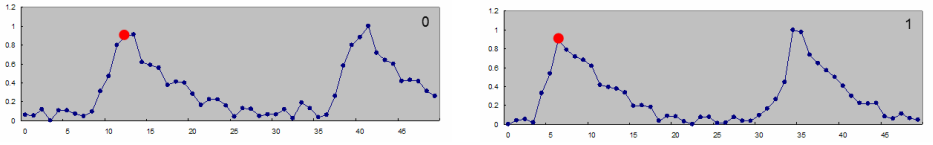

Fig. 4. Respiration signal at two adjacent table positions extracted from swine study. The vertical axis is normalized respiratory phase and the horizontal axis is time in frame number.

signals of two CT fluoroscopy image series obtained in a swine study at two adjacent table positions with an interval of 4mm. It can be observed that the CTF scan time of the two sequences was different with respect to the respiratory cycle. The two dots on the peaks of the respiration signals show the result of synchronization.

After all the 2D image series are synchronized, the 4D lung can be reconstructed by sorting the 2D images. As mentioned in Section 2, the 2D images come from different respiratory cycles. Since the respiratory motion is not completely reproducible, the direct 4D reconstruction by sorting the 2D images can result in very poor image quality. Especially in the coronal and sagittal views, fuzzy edges are usually observed. In response to this problem, we reconstruct the displacement field of the lung volume. In section 2.1, the displacement field of each 2D image has already been calculated from the deformable registration. Each 2D image has also been assigned to a respiratory phase. We generate a displacement field for the entire lung volume by combining the displacement fields of 2D images according to the table position and respiratory phase. The resulting displacement field of the reference volume may not be smooth because it is obtained from different respiratory cycles. However, the displacement field can be smoothed. We use the cubic B-spline [9] to smooth and interpolate the displacement in the cranial-caudal direction to obtain a very smooth displacement for the reference volume. As a result, the 3D volume at any respiratory phase can be computed from a deformable transformation of the reference volume.

3 Experimental Results

We used synthetic 4D data to validate the algorithm. The synthetic 4D data was generated from two lung volumes obtained at the end of inspiration and the end of expiration respectively. The two lung volumes were registered at Siemens Corporate Research using 3D/3D deformable registration. The displacement field between the two volumes was interpolated along the time axis such that the trajectory of each pixel is a 3D curve in space instead of a straight line [11]. The resulting 4D data was used as the ground truth to validate the reconstruction algorithm. The synthetic 2D free scan image series was obtained by sampling the 4D data at the selected table position. With the 2D image series and the lung volume at the end-of-expiration as the reference volume, we ran the algorithm to recover the lung deformation. The pixel size of both the preoperative CT volume and the 2D images was 0.7422mm. The slice thickness of the preoperative CT volume was 1.25mm, and 3.75mm for the synthetic 2D free scan images. The results were first compared to the ground truth to validate the deformable 2D/3D registration.

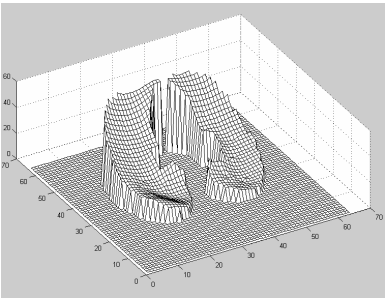

Fig. 5. Displacement magnitude of a CT fluoroscopy image with respect to the reference CT volume in mm

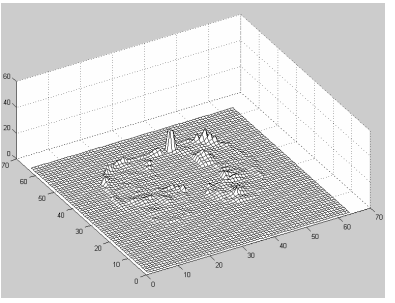

Fig. 6. Magnitude of reconstruction error in mm

Fig. 5 shows the deformation magnitude of a 2D image taken at the end-of-inspiration, when the 2D image has the largest deformation with respect to the reference CT volume. As shown in Fig. 6, most of the poor registrations happen on the boundary pixels of the lung. This problem has three causes. First, for the region-based algorithm, the registration accuracy is usually higher for the pixels near the center of the analysis window. The boundary pixels of lung are usually far from the center of the analysis window. Second, the boundary pixels (especially the boundary pixels near the top of image) have larger deformation than the average. Third, and perhaps most importantly, the areas near the lung boundary often have very little texture information, which may not be enough for the local image registration.

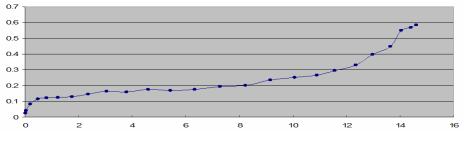

Fig. 7. Average reconstruction error vs. average displacement in mm

Fig. 7 shows the average reconstruction error of the lung pixels compared to the average lung deformation. The maximum average error is 0.6mm. For the respiratory phase with large respiratory motion, the average registration error is below 5% of the average lung deformation.

The algorithm was also tested on the data collected from a swine study as part of an approved animal protocol. This study was done at Georgetown University Medical Center on a Siemens Volume Zoom four-slice CT scanner. The reference volume was obtained at the end-of-expiration using a 1 mm slice thickness. While the animal was mechanically ventilated, for the image acquisition the ventilator was stopped and the animal was temporarily paralyzed to minimize any breathing artifacts. The 2D image series were acquired using CT fluoroscopy with a sample rate of 6Hz and a slice thickness of 4mm. Ten 2D image series were acquired. Fig. 8 and Fig. 9 show the reconstruction results at the end-of inspiration which is the respiratory phase of the maximum deformation with respect to the reference volume. As shown in the figures, the reconstruction result of our algorithm is much smoother compared to the standard image sorting method.

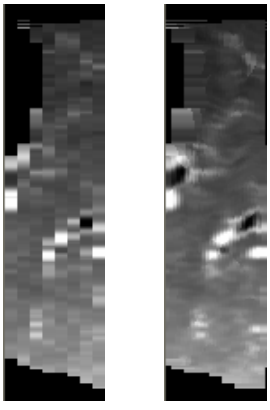

Fig. 8. Sagittal view of 4D reconstruction Left image: image sorting method Right image: our method

Fig. 9. Coronal view of 4D reconstruction Top image: image sorting method Bottom image: our method

4 Discussion and Conclusions

This paper presents a new methodology to reconstruct the 4D lung image. The temporal resolution of the method is high and the reconstruction provides good quality images. Based on a synthetic CT data set, the average reconstruction /registration error is under 5% of the average lung deformation, which is less than or equal to 0.6mm of respiratory motion. Results from a swine study also showed good correlation.

The algorithm is automated and software based. The algorithm does not need any auxiliary surrogates to synchronize the CT scan with the respiratory phase. The image reconstruction quality of the algorithm is very high even under irregular respiratory motion. The drawback of the algorithm is that it is time consuming. It takes about 5 minutes to register each 2D image to the reference volume. If improved processing speed is needed, the algorithm can be implemented on a parallel processing machine.

Although the algorithm was only tested on the synthetic data of the single slice CT and in one swine study, it can be easily extended for use with multi-slice CT. Since multi-slice CT allows the local region registration to have more texture information, it is expected to see higher accuracy and better robustness of the algorithm.

Acknowledgement. The authors gratefully thank Frank Sauer, Ph.D., Ali Khamene, Ph.D. and Christophe Chefd'hotel, Ph.D. at Siemens Corporate Research for providing the lung dataset. The dataset was originally obtained by the EMC in Rotterdam. The authors also thank David Lindisch, RT, for his assistance with the experiments at Georgetown University. The work was supported by U.S. Army grants DAMD17-99-1-9022 and W81XWH-04-1-0078, NSF Engineering Research Center 9731478.

References

1. Keall, P.: 4-dimensional computed tomography imaging and treatment planning. Semin Radiat Oncol. 14 (2004) 81-90
2. El Naqa, I. M., Low, D. A., Christensen, G. E., Parikh, P. J., Song, J. H., Nystrom, M. M., Lu, W., Deasy, J. O., Hubenschmidt, J. P., Wahab, S. H., Mutic, S., Singh, A. K., Bradley, J. D.: Automated 4D lung computed tomography reconstruction during free breathing for conformal radiation therapy. In: Amini, A. A., Manduca, A. (eds.): Medical Imaging 2004: Physiology, Function, and Structure from Medical Images, Vol. 5369. SPIE (2004) 100-106
3. Boldea, V., Sarrut, D., Clippe, S.: Lung Deformation Estimation with Non-rigid Registration for Radiotherapy Treatment. In: Ellis, R. E., Peters, T. M. (eds.): Medical Image Computing and Computer-Assisted Intervention. Lecture Notes in Computer Science, Vol. 2878. Springer-Verlag GmbH (2003) 770-777
4. Vedam, S. S., Keall, P. J., Kini, V. R., Mostafavi, H., Shukla, H. P., Mohan, R.: Acquiring a four-dimensional computed tomography dataset using an external respiratory signal. Phys Med Biol. 48 (2003) 45-62
5. Underberg, R. W., Lagerwaard, F. J., Cuijpers, J. P., Slotman, B. J., van Sornsen de Koste, J. R., Senan, S.: Four-dimensional CT scans for treatment planning in stereotactic radiotherapy for stage I lung cancer. Int J Radiat Oncol Biol Phys. 60 (2004) 1283-90
6. Pan, T., Lee, T. Y., Rietzel, E., Chen, G. T.: 4D-CT imaging of a volume influenced by respiratory motion on multi-slice CT. Med Phys. 31 (2004) 333-40
7. Ford, E. C., Mageras, G. S., Yorke, E., Ling, C. C.: Respiration-correlated spiral CT: a method of measuring respiratory-induced anatomic motion for radiation treatment planning. Med Phys. 30 (2003) 88-97
8. Xu, S., Fichtinger, G., Taylor, R. H., Cleary, K. R.: 3D motion tracking of pulmonary lesions using CT fluoroscopy images for robotically assisted lung biopsy. In: Galloway, R. L., Jr. (ed.): Medical Imaging 2004: Visualization, Image-Guided Procedures, and Display, Vol. 5367. SPIE (2004) 394-402
9. Unser, M.: Splines - A perfect fit for signal and image processing. Ieee Signal Processing Magazine. 16 (1999) 22-38
10. Hu, S., Hoffman, E. A., Reinhardt, J. M.: Automatic lung segmentation for accurate quantitation of volumetric X-ray CT images. IEEE Trans Med Imaging. 20 (2001) 490-8
11. Xu, S., Fichtinger, G., Taylor, R. H., Cleary, K. R.: Validation of 3D motion tracking of pulmonary lesions using CT fluoroscopy images for robotically assisted lung biopsy. In: Galloway, R. L., Jr., Cleary, K. R. (eds.): Medical Imaging 2005: Visualization, Image-Guided Procedures, and Display, Vol. 5744. SPIE (2005) 60-68